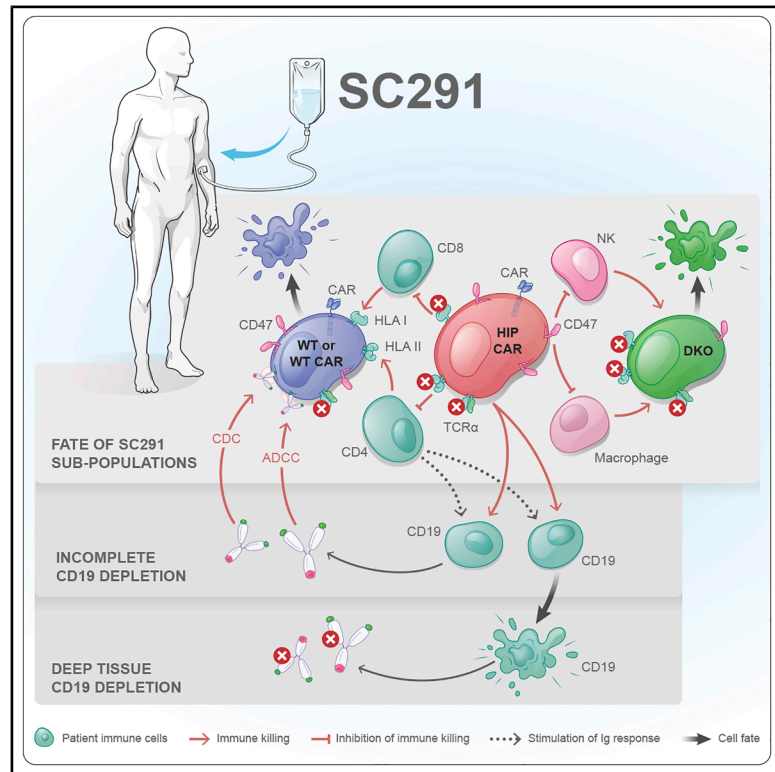


### Hypoimmune CD19 CAR T cells evade allorejection in patients with cancer and autoimmune disease

#### Graphical abstract



#### Authors

Xiaomeng Hu, Pascal Beauchesne, Chenyan Wang, Athena Wong, Tobias Deuse, Sonja Schrepfer, ARDENT and GLEAM investigators

#### Correspondence

sonja.schrepfer@sana.com

#### In brief

Schrepfer and colleagues investigated the immune response against subpopulations of the hypoimmune, allogeneic CD19 CAR T cell product SC291 in clinical trials. Although patients mounted a rejection response against unedited or partially edited T cells, fully edited hypoimmune CAR T cells with HLA depletion and CD47 overexpression were not attacked.

#### Highlights

- HIP CAR T cells exhibit HLA depletion and CD47 overexpression
- Allogeneic HIP CAR T cells do not induce an immune response in patients
- Patients with deep tissue B cell depletion lack *de novo* antibody production

## Clinical and Translational Report

# Hypoimmune CD19 CAR T cells evade allorejection in patients with cancer and autoimmune disease

Xiaomeng Hu,<sup>1</sup> Pascal Beauchesne,<sup>1</sup> Chenyan Wang,<sup>1</sup> Athena Wong,<sup>1</sup> Tobias Deuse,<sup>1,2</sup> Sonja Schrepfer,<sup>1,4,\*</sup> and ARDENT and GLEAM investigators<sup>3</sup>

<sup>1</sup>Sana Biotechnology Inc., 1 Tower Place, South San Francisco, CA, USA

<sup>2</sup>Present address: Department of Surgery, Division of Cardiothoracic Surgery, Transplant and Stem Cell Immunobiology (TSI)-Lab, University of California, San Francisco, San Francisco, CA, USA

<sup>3</sup>The investigators, institutions, and research organizations participating in the ARDENT and GLEAM trials are listed in the supplemental information

<sup>4</sup>Lead contact

\*Correspondence: sonja.schrepfer@sana.com

<https://doi.org/10.1016/j.stem.2025.07.009>

## SUMMARY

Off-the-shelf CAR T cells need to reliably escape allogeneic immune responses to become universal medicines. The primary T cell product SC291 was engineered with a CD19 CAR, T cell receptor alpha constant (TRAC) knockout, and the hypoimmune (HIP) edits of HLA depletion and CD47 overexpression. Here, we report exploratory immune analyses from the ARDENT (NCT05878184) and GLEAM (NCT06294236) trials with HIP-edited CD19 CAR T cells. Although there was an alloimmune response against HLA-replete subpopulations of SC291, we observed no *de novo* immune response against fully edited HIP CAR T cells in all patients, irrespective of the dose or the patient's disease. The lack of antibodies against the HLA-replete CAR T cells was identified as a marker for deep tissue CD19 cell depletion, and all patients without such antibodies for 60 days showed concomitant B cell depletion in peripheral blood. The immune data presented support the reliability of the HIP concept to evade allorejection.

## INTRODUCTION

Allogeneic cell therapeutics combine multiple advantages over autologous products, including expedient manufacturability from highly selected healthy donor cells, scalability, and cost efficiency.<sup>1,2</sup> The susceptibility of allogeneic cells to immune rejection in human leukocyte antigen (HLA)-discordant patients, however, dramatically limits their efficacy and has so far largely diminished their success in clinical trials.<sup>3–5</sup> The required aggressive immunosuppression for regenerative cell replacement therapies like islet cells for diabetes mellitus<sup>6,7</sup> or cardiomyocytes for heart failure<sup>8</sup> dampens the enthusiasm and reduces their acceptance due to the risk for serious immunosuppressive-drug-related side effects. Similarly, intensified protocols for lymphodepleting preconditioning for immune-oncology products like CAR T cells were associated with an increase in the rate of infections while still proving inadequate for therapeutic potency.<sup>9</sup> There has thus been a major research effort in recent years to develop strategies that allow allogeneic cells to subvert allorecognition in immunocompetent patients or even enable cells to evade pre-existing or ongoing alloreactivity.<sup>10–14</sup> Our group developed the hypoimmune (HIP) concept that includes the depletion of class I and II HLA and the overex-

pression of CD47<sup>15</sup> at levels that are protective against innate immune cell killing.<sup>16</sup> In preclinical studies, we could confirm that HIP-engineered human primary islets,<sup>17</sup> as well as islets differentiated from human HIP induced pluripotent stem cells (iPSCs),<sup>18</sup> were fully immune evasive and capable of surviving and treating diabetes in allogeneic, diabetic humanized mice. Furthermore, human HIP-engineered primary CD19 CAR T cells were shown to engraft in allogeneic, humanized mice and control Nalm6 cancers.<sup>19</sup> HIP CAR T cell persistence in the bone marrow and lymphatic organs was achieved and their continued functionality was demonstrated by their expeditious elimination of re-injected cancer cells 3 months later.<sup>19</sup> In-depth immune analyses in all these studies with immunocompetent, humanized mice corroborated that HIP cells do not induce any immune response and effectively escape all cellular rejection responses. Subsequent translational studies, first with allogeneic HIP iPSCs<sup>18</sup> and later with allogeneic primary HIP islets in non-human primates,<sup>18,20</sup> confirmed their reliable immune-evasive character as evidenced by their ability for long-term survival in the complete absence of any alloimmune activation. The HIP concept of immune engineering holds promise for a new generation of universal cell therapeutics in regenerative medicine as well as immune cell therapy for cancer and



**Table 1. Drug product characteristics**

SC291 drug product	
Attributes	Frequency
Viability	90.7%
CAR+ cells	55.8%
CD47-high cells	55.4%
HLA-ABC depletion	91.1%
HLA-DR, DP, DQ depletion	91.5%
TCR $\alpha\beta$ + cells	<0.2% (LLOQ)
CD4+ cells	55.4%
CD8+ cells	41.2%
HIP CAR T cells	40.9%

Attributes of the SC291 drug product are shown for the lot used in this study. Frequencies were generated through flow cytometry. LLOQ, lower limit of quantitation. The frequency of HIP CAR T cells was measured by direct flow co-gating for live TCR-negative, HLA-ABC-negative, HLA-DR, DP, DQ-negative, CD47 high, and CD19 CAR-positive cells.

autoimmunity. We herein report the reliability of the HIP engineering concept in a HIP CAR T cell product employed in two first-in-human studies.

The potential of CD19-directed CAR Ts to deplete B cells has shown promise in two main clinical applications to date: the elimination of malignant B cells in leukemia and lymphoma and the suppression of autoantibodies in autoimmune diseases. Although depletion of circulating B cells may transiently improve symptoms in autoimmune patients, it is thought that a deeper B cell depletion is necessary to achieve “immune reset” and durable clinical improvements. It is therefore helpful to determine the depth and duration of B cell depletion during the development of new therapies. This has historically been done by demonstrating depletion of B cells in lymph node biopsies in patients. Our HIP platform has the potential for a unique, non-invasive way to assess deep B cell depletion using patient serum samples. Immune data from two clinical trials were pooled to assess the immunology of HIP CD19 CAR T cells in a disease-agnostic manner.

## RESULTS

### Patients

Data from 14 patients enrolled in the ARDENT trial (NCT05878184) and one patient enrolled in the GLEAM trial (NCT06294236) were available at the exploratory immune data cutoff date of September 19, 2024 (Table S1). No data obtained after that were included in this analysis. One patient in ARDENT withdrew consent for exploratory research and was excluded from this analysis, leaving 14 patients for this immune study. All patients in ARDENT received low-dose lymphodepleting chemotherapy consisting of cyclophosphamide 500 mg/m<sup>2</sup> and fludarabine 30 mg/m<sup>2</sup> daily for 3 days, and the patient in GLEAM received one dose of cyclophosphamide 1,000 mg/m<sup>2</sup> and three daily doses of fludarabine 25 mg/m<sup>2</sup>. The SC291 dose levels for patients in ARDENT ranged from 60 to 200 million CAR T cells, and the patient in GLEAM received 90 million CAR T cells. All patients had blood drawn at baseline on day –5, before undergoing lymphodepletion and the infusion of the CAR T cell product. At several time points after CAR T cell admin-

istration, blood and serum were drawn for in-depth immune analyses of the adaptive cellular immune response, humoral immune response, and innate immune response.

### CD19 CAR T cells

SC291 is a HIP, CD19-directed, allogeneic CAR T cell product that is derived from healthy donor T cells, including both CD8+ and CD4+ populations (Table 1). CRISPR-Cas editing was performed to disrupt the T cell receptor alpha constant (*TRAC*), beta-2-microglobulin (*B2M*), and class II major histocompatibility complex transactivator (*CIITA*) genes. Overexpression of CD47 and expression of a CD19-directed CAR was achieved with a bicistronic lentiviral vector. All patients in this study received their product from the same batch. Manufacturing generated a mix of (1) partially edited wild-type (WT) T cells with retained HLA, TCR depletion, and with or without CD19 CAR expression and CD47 overexpression; (2) partially edited DKO cells with HLA and TCR depletion, but without expression of the CD19 CAR-CD47 expression cassette; and (3) fully edited HIP CAR T cells (Figures 1A and 1B). Approximately 40.9% of cells were fully edited HIP CAR T cells (Figure 1C; Table 1). The residual TCR frequency was less than 0.2%. Because these cells were not sorted before infusion, patients received a therapeutic product that contains a mixture of WT and HIP CAR T cells and DKO cells.

### Overall immune analysis

Because of the unique mixture of cells infused into patients treated with SC291, we were able to assess immune reactions separately to the three main populations of T cells in our product (WT CAR T cells, HIP CAR T cells, and DKO cells). Three patients treated in these studies had pre-existing antibody-mediated baseline killing of HIP CAR T cells *ex vivo*, and those patients are described in detail below. These patients were excluded from the overall immune analysis, leaving 11 patients for the remaining analysis. Striking similarities in the immune responses of these 11 patients were observed irrespective of their underlying diagnoses or CAR T cell dose. No patient showed a T cell enzyme-linked immunospot (ELISpot) response against HIP CAR T cells during baseline assessment or at any time point after SC291 administration (Figure 2A). Correspondingly, there was no T cell cytotoxicity against HIP CAR T cells in any of these patients during the entire period studied (Figure 2B). Similar results were obtained with HLA class I- and II-depleted DKO cells. Although none of these patients showed T cell activity or cytotoxicity against WT CAR T cells at baseline, all patients were immunized against allogeneic HLA and responded with a typical interferon (IFN)- $\gamma$  response that peaked at 28 days after CAR T cell administration (Figures 2A and 2B). All patients developed T cell cytotoxicity against WT CAR T cells and showed WT CAR T cell killing at all time points after receiving SC291. HIP and WT CAR T cells (both of which overexpress CD47) were completely protected from killing by interleukin-2 (IL-2)-activated natural killer (NK) cells, but DKO cells (which lack CD47 overexpression) were killed at baseline and all time points thereafter in these patients (Figure 2C). No donor-specific antibodies (DSAs) were generated against HIP CAR T cells or DKO cells in these patients during this study (Figure 2D). Together, these immune data show that the HIP fraction of SC291 was fully immune evasive in all patients, irrespective of their diagnosis or CAR

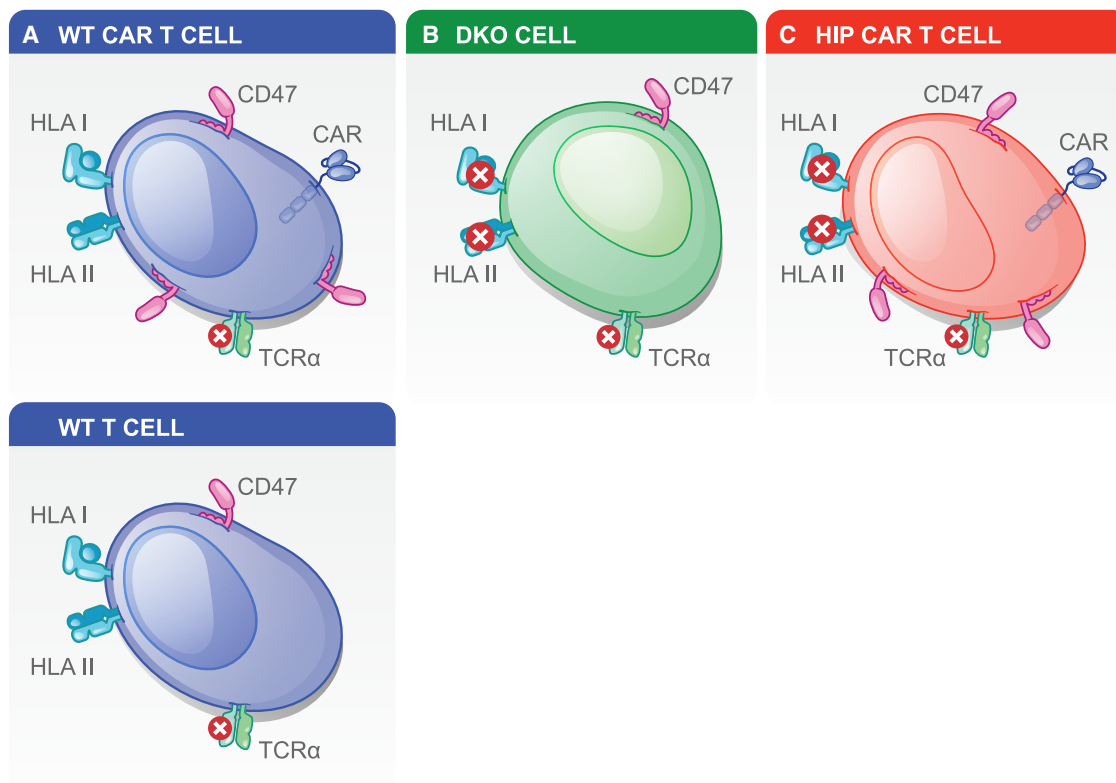


**Figure 1. Composition of SC291**

(A–C) Primary T cells were isolated from donor leukopaks; *B2M*, *CITA*, and *TRAC* were inactivated using CRISPR and Cas12b; and a CD19 CAR and CD47 were then transduced using a bicistronic lentivirus. This protocol generated a mixture of HLA-replete WT T cells and CAR T cells (A), DKO cells (B), and fully edited HIP CAR T cells (C).

T cell dose. The ability of patients to turn their T cell activation against WT CAR T cells into a B cell response is shown in the subgroup analyses below.

#### Subgroup analyses

The presence of CD19 B cell depletion in the peripheral blood has previously been shown to serve as a surrogate to gauge the functional persistence of CD19 CAR T cells.<sup>21</sup> In some patients, CD19 cell markers were suppressed but never dropped below the detection level. Other patients achieved transient CD19 marker depletion, but CD19 cell markers re-emerged later. Durable CD19 marker depletion was attained in several patients throughout the study period.

#### Patients who never achieved CD19 depletion

Two patients were included in this subgroup. Both showed a reduction in peripheral blood CD19-positive cells during follow-up, but CD19 remained detectable at all time points (Figure 3A). IgE levels, which were used as indicator for immuno-globulin production, showed only a very mild, temporary reduction in these patients, suggesting persistence of their corresponding antibody-producing cells (Figure 3B). Both patients developed DSAs against WT CAR T cells, which persisted throughout the observation period (Figure 3C). No DSAs were generated against HIP CAR T cells or DKO cells. Patients mounted a T cell response with T cell cytotoxicity against WT CAR T cells but not against HIP CAR T cells or DKO cells

(Figures 3D and 3E). Only DKO cells were susceptible to NK cell killing (Figure 3F). The surge in DSAs against WT CAR T cells led to NK cell antibody-dependent cell-mediated cytotoxicity (ADCC) and complement-dependent cytotoxicity (CDC) against WT CAR T cells during all time points after the SC291 administration (Figures 3G and 3H). DKO cells were not killed in NK cell ADCC assays because NK cells were not IL-2 activated and were thus missing the additional stimulatory signal when no antibodies bound the target cells.<sup>16</sup> Also, no HIP cells were killed in ADCC or CDC assays. The main observations in this subgroup include the persistence of CD19 cells in the blood and the ability of the patients to mount an antibody response against WT CAR T cells, which corresponded with antibody-mediated killing of WT CAR T cells through both effector immune cells and complement. These two patients had by far the highest CD19 burdens among all patients in this study.

#### Patients with transient CD19 depletion

In this subgroup of three patients, transient CD19 depletion was achieved in peripheral blood, but CD19 cells came back at later time points (Figure 4A). IgE levels dropped, became temporarily undetectable in two patients, but were then detectable at later time points in all patients at low levels (Figure 4B). DSAs against WT CAR T cells were detectable in all patients during the follow-up (Figure 4C; above background levels). No DSAs bound to HIP CAR T cells or DKO cells. We again observed the typical adaptive T cell response against WT CAR T cells and the killing of DKO

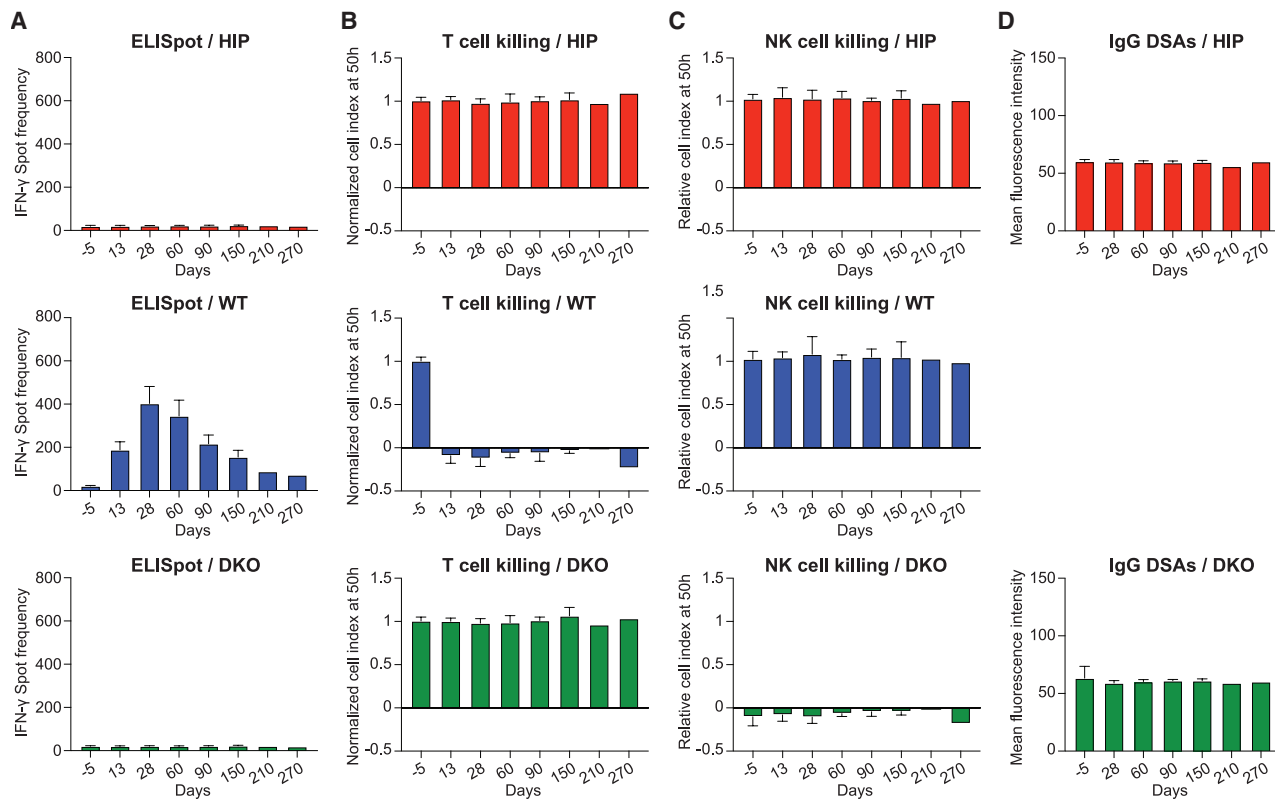


**Figure 2. Overview of immune response of 11 patients**

Immune response data for 11 patients were summarized.

(A) IFN- $\gamma$  ELISpot data from patient peripheral blood T cells showed no activation by HIP CAR T cells or DKO cells but strong activation by WT CAR T cells, with peak spot frequency at 28 days.

(B) No T cell killing of HIP CAR T cell or DKO cell targets was observed at any time point in any patient. However, activated T cells killed the WT CAR T cell fraction in all patients at all time points after they received the SC291 product.

(C) No NK cell killing of HIP CAR T cells or WT CAR T cells was observed in any patient, but DKO cells were reliably killed in all patients at all time points.

(D) No IgG DSAs against HIP CAR T cells or DKO cells were detected in any patient. Bar graphs show mean  $\pm$  SD.

cells by NK cells (Figures 4D–4F). During all time points when DSAs were detectable against WT CAR T cells, we also observed ADCC and CDC against the WT targets. Only one marginal DSA binding in one patient (blue patient) at day 28 did not result in ADCC and CDC killing of WT CAR T cells, suggesting these newly developed low-level antibodies were not cytotoxic yet. No ADCC and CDC against WT CAR T cells was seen when no DSAs were present (Figures 4G and 4H). This tight correlation supports the validity of these assays and shows that DSAs in all patients became cytotoxic in nature.

#### Patients with durable CD19 depletion

This group comprises six patients. Peripheral blood CD19 cells dropped below the detection level and remained undetectable throughout the follow-up period (Figure 5A). IgE levels dropped below the detection level in three patients and remained undetectable thereafter. In another three patients, IgE dropped close to the detection level but remained detectable at very low levels and showed no tendency for increase (Figure 5B). In this subgroup, no DSAs against WT CAR T cells could be observed at any time point after SC291 administration (Figure 5C). Because all patients in this subgroup mounted a similar T cell response with T cell cytotoxicity against WT CAR T cells that was also

seen in the other groups, the complete lack of DSAs hints at an isolated inability to generate IgG despite robust T cell activation (Figures 5D and 5E). This suggests broad deep tissue depletion of CD19 cells in otherwise immunized patients. A lack of DSAs against the WT CAR T cell fraction thus appears to be the most accurate marker for deep tissue depletion of antibody-producing cells. Although antibody-producing cells in lymphoid tissue might remain undetectable in peripheral blood CD19 counts, their antibodies against the WT CAR T cell fraction might be a sensitive way to detect non-circulating CD19 cells. The DKO cell fraction was killed by NK cells at all time points, thus confirming their functionality throughout the study (Figure 5F). Due to the complete absence of DSAs against WT CAR T cells, we observed no ADCC or CDC killing against WT targets (Figures 5G and 5H).

#### SC291 CD19 CAR T cell efficacy

Because of the staggered patient enrollment during dose escalation, patients in the higher-dose groups had a shorter follow-up. To allow correlations with SC291 dose levels, we combined the 60 and 90 M patients into the low-dose group and defined 120 M as the medium- and 200 M as the high-dose group.

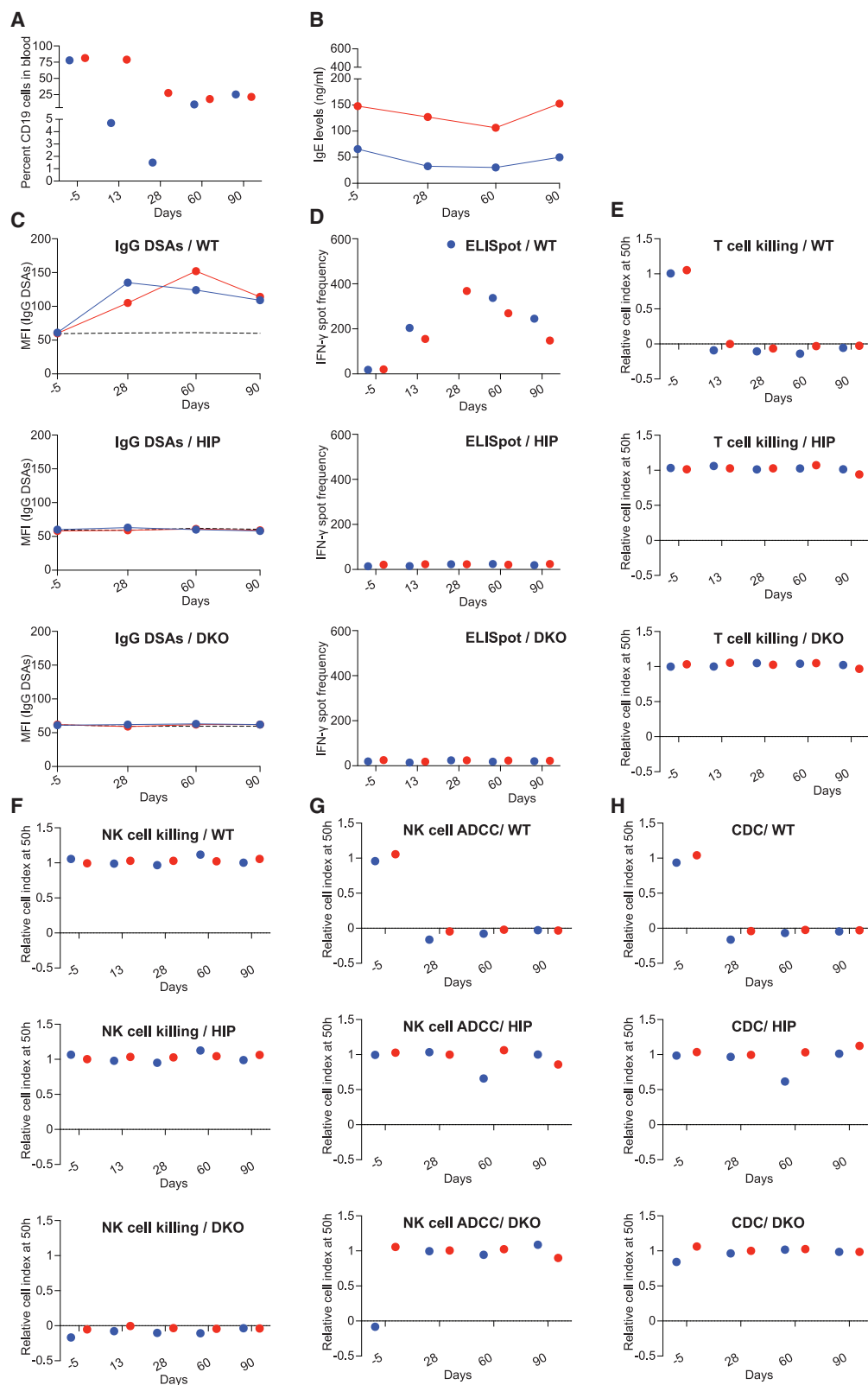


**Figure 3. Patients who never achieved CD19 depletion**

(A) The percentages of CD19 cells in peripheral blood throughout the study are shown.  
(B) Circulating IgE levels are shown over time.

(legend continued on next page)

Similar group sizes were available when focusing on a 2-month follow-up period; one patient with only a 1-month follow-up was excluded. Only one out of three patients in the low-dose group maintained complete B cell depletion in peripheral blood at day 60, two of three patients in the 120 M group, and all four patients in the 200 M group (Figure S1A). There was a dose-dependent effect when evaluating the efficacy of SC291 to suppress WT DSAs for 2 months. Although this was not achieved in any low-dose patient, two out of three patients in the 120 M group and all four patients in the 200 M group showed deep tissue B cell depletion without occurrence of WT DSAs by day 60 (Figure S1B). Although there were two patients with very high CD19 cell burden at baseline, there was no statistically significant difference in CD19 burden between patients that did and did not show effective WT DSA suppression with SC291 (Figure S1C). Although only one out of four patients who did not show WT DSA suppression for 2 months achieved complete B cell depletion in peripheral blood at day 60, all six patients with effectively suppressed WT DSAs did (Figure S1D).

#### Patients with baseline killing of HIP CAR T cells

Serum from three patients showed baseline rejection of HIP cells. In these 3 patients, dosing with SC291 showed no effect on IgE levels at any time points tested (Figure 6A). Two patients showed baseline antibody binding against all three fractions of SC291, including WT CAR T cells, HIP CAR T cells, and DKO cells (Figures 6B and 6H). All of those DSAs were shown to be cytotoxic and ADCC and CDC assays demonstrated the killing of all three cell fractions in both patients (Figures 6C, 6D, 6I, and 6J). Both patients had pre-formed antibodies against the SC291 product that were directed against non-HLA epitopes because HLA-replete WT CAR T cells and HLA-depleted HIP CAR T cells and DKO cells were similarly affected. These patients showed no T cell or NK cell response that was qualitatively different from all other patients (Figures 6E–6G and 6K–6M). Because one of these patients (the second patient) showed a positive Coombs test, additional CDC assays were performed with patient serum on blood group O endothelial cells (ECs) that were either negative or positive for the rhesus blood group antigen Rh(D) (Figure S2). The serum of the first patient killed both ECs and was thus directed against a different common antigen on both ECs. Serum from the second patient with positive Coombs test selectively killed Rh(D)-expressing ECs and suggests that anti-Rh(D) antibodies may have caused the observed baseline killing. The third patient did not show baseline DSAs against any of the SC291 subpopulations with our general setup using a secondary antibody with preferred affinity for human IgG1 (Figure 6N). The patient's history, however, revealed that he was treated with the recombinant signal regulatory protein  $\alpha$

(SIRP $\alpha$ )-IgG4 fusion protein TTI-622 before being enrolled in this study. When a secondary antibody specifically binding human IgG4 was used instead, DSAs against both the WT CAR T cell and HIP CAR T cell fractions, but not DKO cells, were observed (Figure 6O). Accordingly, we saw ADCC baseline killing of the WT and HIP CAR T cells but not of the DKO cells (Figure 6P). When recombinant CD47 was added to the ADCC assays with WT or HIP CAR T cells to saturate the SIRP $\alpha$ -IgG4 fusion protein, then no more ADCC killing was seen (Figure 6Q). We did not observe CDC killing of WT or HIP CAR T cells (Figure 6R). The T cell and NK cell responses in this patient were in line with those of all the other patients (Figures 6S–6U). To assess the ADCC killing capacity of TTI-622 against the three SC291 subpopulations *in vitro*, increasing SIRP $\alpha$ -IgG4 concentrations were tested (Figure S3). TTI-622 was cytotoxic in a concentration-dependent manner only against the WT and HIP CAR T cell fractions with elevated CD47 expression but not against DKO cells with endogenous expression levels.

#### DISCUSSION

This is the first report demonstrating the reliable immune-evasive capacity of allogeneic HIP immune cells in patients. The immune assays presented herein cover the activation and response of the patients' T cells as well as their innate NK cells and macrophages. Additionally, we screened for the emergence of *de novo* antibodies against the subpopulations of SC291 and correlated them with antibody-mediated cytotoxicity assays. HIP cells did not induce any *de novo* cellular or humoral immune response in any patients at any time point. The same immune assays had previously shown that monkey HIP cells were fully protected against all allogeneic adaptive and innate immune cell killing in non-human primates.<sup>18,20</sup> This first human study corroborates those previous findings and elucidates the robustness of the HIP concept in patients. Given the remarkable degree of NK cell diversity, with an estimated 6,000–30,000 phenotypic populations within any individual and the enormous heterogeneity across a population,<sup>22</sup> the universal potency of the inhibitory CD47-SIRP $\alpha$  pathway is noteworthy. Active NK cell cytotoxicity against DKO T cells was confirmed in all patients and supports the overall functional competence of NK cells even after lymphodepletion.

HIP engineering of primary cells inevitably produces fractions of partially edited cells, and the immune response against the SC291 CAR T cell product was assessed separately for all cell fractions. Patients receiving SC291 were actively immunized against the HLA of the WT CAR T cells, and a corresponding immune response against WT cells was observed in all patients. The lack of an enhanced lymphodepletion regimen used in this

(C) IgG DSAs against the three cell fractions of SC291 were quantified by flow cytometry and expressed as MFI.

(D) Patient T cell activation by the three cell fractions of SC291 was assessed in ELISpot assays and is expressed as spot frequency.

(E) The cytotoxicity of patient T cells against the three cell fractions of SC291 was assessed in impedance cytotoxicity assays.

(F) The cytotoxicity of patient NK cells against the three cell fractions of SC291 was assessed in impedance cytotoxicity assays.

(G) For ADCC assays against the three cell fractions of SC291, patient NK cells and serum were combined and killing was assessed in impedance cytotoxicity assays. In one patient (blue), the NK cells at day –5 were endogenously activated to kill DKO cells even without serum; therefore, this outlier is not an indication of the presence of antibodies.

(H) For CDC assays against the three cell fractions of SC291, patient serum was used in impedance cytotoxicity assays. This group comprised 2 patients. Patients are color coded and all individual patient data are shown.

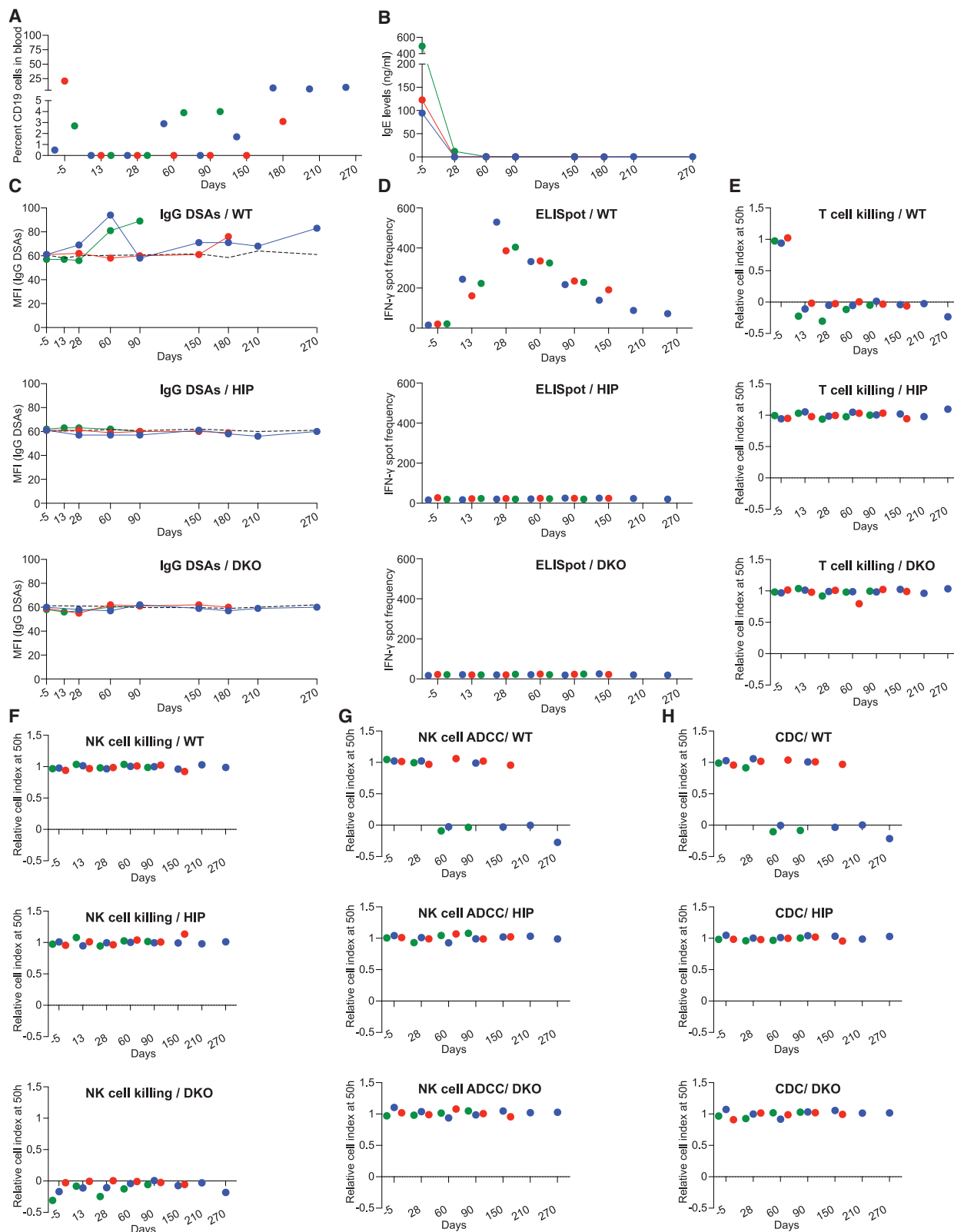


**Figure 4. Patients with transient CD19 depletion**

(A) The percentages of CD19 cells in peripheral blood are shown.  
(B) Circulating IgE levels are shown over time.

(legend continued on next page)

study allowed an early induction of an appropriate T cell response against the WT HLA on day 13. The peak of T cell activation was at 28 days and T cell activation correlated with T cell cytotoxicity against WT targets in all patients at all time points. Similarly, DKO cells were susceptible to NK cell killing, and NK cells at day 13 were able to kill DKO targets. Lymphodepletion therefore also did not markedly weaken the patient's innate immune response. However, no T cell or NK cell killing of HIP CAR T cells was observed in any patient or at any time point. HIP cells therefore did not only avoid the induction of any *de novo* immune response but were also not susceptible to the ongoing rejection responses against the other cell fractions. We had previously observed the same protection of HIP stem cells in non-human primates during times when the same animals rejected subsequently injected MHC-replete WT cells.<sup>18</sup> Similarly, when Nalm6 tumor-bearing, allogeneic humanized mice were treated with SC291, which has approximately 40.9% HIP CAR T cells, all other CAR T phenotypes were rejected over time and, after 95 days, all CAR-positive cells in those mice were HIP T cells.<sup>19</sup> HIP cells thus seem unaffected by ongoing rejection of other unedited or partially edited cell fractions in preclinical studies. HIP CAR T cell persistence in patients remains to be shown.

The absence of CD19 cells in peripheral blood is used as a biomarker for the efficacy of the CD19 CAR T cell product. However, a biomarker that indicates a more complete depletion of B cells would be desirable because the majority of CD19 cells are located within the bone marrow and germinal centers of secondary lymphoid organs,<sup>23</sup> which are not immediately accessible for detection. Immunoglobulin levels, as products of antibody-producing cells, might be additional parameters for deep tissue depletion. In this study, IgE levels were found to drop to the level of detection within 28 days of CD19 CAR T cell therapy in those patients who showed CD19 depletion in peripheral blood at this time. In patients that never achieved CD19 depletion, IgE levels barely changed. However, while IgE was a good marker for initial CD19 depletion, its levels remained low despite the re-emergence of CD19 cells. We here suggest DSAs against the WT CAR T cell fraction as potential markers for deep tissue depletion of CD19 cells. Because activation of T cells is a strong driver toward the generation of DSAs, only a drastic decimation of CD19 cells in lymphoid organs can prevent their production. In patients that achieved CD19 depletion in peripheral blood but had reoccurrence of CD19 cells later, DSAs against WT CAR T cells consistently emerged at least one time point earlier than the detected reoccurrence of CD19 cells in the blood. DSAs against WT CAR T cells were thus descriptive of deep tissue depletion of CD19 cells and their emergence might be predictive of a patient's relapse.

Pre-formed antibodies against the cell product SC291 were identified as an important hurdle to consider for HIP CAR T cell survival. Of the two patients with pre-formed antibodies cytotoxic for all three cell fractions, one showed selectivity for Rh(D)-blood-group-expressing target cells. In another patient, the antibodies led to the selective killing of the CD47-overexpressing WT and HIP CAR T cells. The patient had received 2 cycles of the SIRP $\alpha$ -IgG4 fusion protein TTI-622 5 months prior to SC291 infusion. The IgG4 isotype of the DSAs could be identified, and the cytotoxicity in ADCC assays could be averted by saturating the DSAs with recombinant CD47. TTI-622-mediated killing specific for CD47-overexpressing target cells could be verified *in vitro*. It is thus possible that persistence of this fusion protein mediated this baseline killing. IgG4 has been shown to have somewhat low binding affinity to Fc $\gamma$ RIIa on NK cells<sup>24,25</sup> and extremely low affinity to complement.<sup>26,27</sup> That could explain why cytotoxicity could only be observed with high CD47 expression and only in ADCC assays. Because no baseline testing was performed prior to enrollment, the three patients with baseline killing were not identified before the initiation of treatment. All three patients showed no change in IgE levels, which points to the persistence of antibody-producing cells and the lack of CAR T cell efficacy. The prevalence of patients having pre-formed antibodies against their allogeneic CAR T cell product is largely unknown and not regularly assessed in clinical trials. Similar patients in other studies would most likely simply be labeled as non-responders, and the reason for the failure of their CAR T cell product would remain unknown. We believe blood group compatibility should be considered for all cell therapy applications. The implementation of testing akin to a blood transfusion could identify such patients and exclude them early on.

This pooled interim analysis of patients with both malignant and benign diseases receiving SC291 supports the reliability of the HIP concept to evade allogeneic cellular immunity. The long-term fate of allogeneic CAR T cells that excite no immune response is likely more influenced by their cellular fitness and their propensity for exhaustion than by immune rejection.<sup>28,29</sup> Central memory and stem cell memory CAR T cells have shown stronger expansion potential and longer persistence than effector CAR T cells.<sup>30</sup> Ultralong CAR T cell persistence was observed with enriched T helper two functionality, which balanced functional homeostasis and optimal fitness of the whole CAR T cell population.<sup>21,31</sup> Cellular fitness can further be enhanced through the knockout of genes, including *PDCD1*,<sup>32</sup> *TGFBR2*,<sup>33</sup> and *ZC3H12A*.<sup>34</sup> These encouraging immune data give confidence that the immune rejection barrier of allogeneic cell therapeutics can reliably be overcome, and more universal HIP cell products could be emerging.

(C) IgG DSAs against the three cell fractions of SC291 were quantified by flow cytometry and expressed as MFI.

(D) Patient T cell activation by the three cell fractions of SC291 was assessed in ELISpot assays and is expressed as spot frequency.

(E) The cytotoxicity of patient T cells against the three cell fractions of SC291 was assessed in impedance cytotoxicity assays.

(F) The cytotoxicity of patient NK cells against the three cell fractions of SC291 was assessed in impedance cytotoxicity assays.

(G) For ADCC assays against the three cell fractions of SC291, patient NK cells and serum were combined and killing was assessed in impedance cytotoxicity assays.

(H) For CDC assays against the three cell fractions of SC291, patient serum was used in impedance cytotoxicity assays. This group comprised 3 patients. Patients are color coded and all individual patient data are shown.

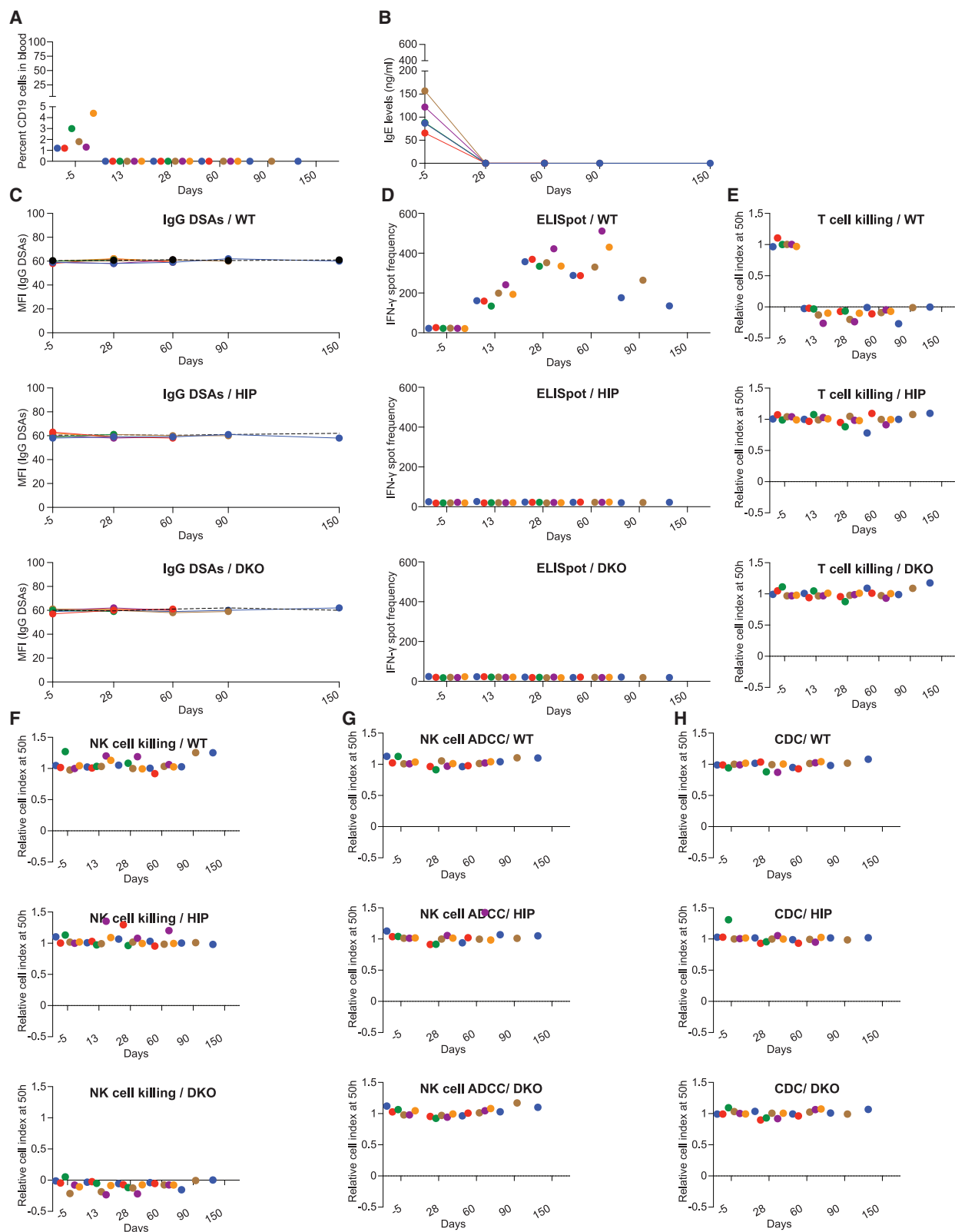


**Figure 5. Patients with durable CD19 depletion**

(A) The percentages of CD19 cells in peripheral blood are shown.  
(B) Circulating IgE levels are shown over time.

(legend continued on next page)

### Limitations of the study

This study focuses on the immune response of patients against SC291 and does not report safety or primary efficacy outcome measures of ARDENT or GLEAM. In-depth immune analyses of 14 patients are reported herein, and subgroups were defined based on differences in achieving CD19 depletion. Group sizes were between 2 and 6 patients and the conclusions derived are based on limited data and need to be interpreted with caution. That is despite the fact that patients within individual groups were consistently very homogeneous. The follow-up period varies between groups and is shorter in the patient cohort with durable CD19 depletion due to the stagger in enrollment for the different dose levels. Therefore, many subjects in the high-dose level have a shorter follow-up than lower-dose levels and no conclusions about durability can be made. However, the peak of the immune rejection response to HLA-replete CAR T cells is early, around day 28, and the complete absence of adaptive or innate responses against the HIP CAR T cells in all patients of all groups strongly supports the reliability of the HIP immune evasion concept. HIP CAR T cell data will be reported with the official study reports and were not available for this interim analysis, which focuses on the immunology of SC291. Although allorejection is generally considered a potential limiting factor for the persistence of allogeneic cell products, many other factors outside of the immunology, including cellular fitness, molecular determinants, exhaustion, and T cell stemness, also play important roles. The persistence of autologous CAR T cells also differs based on disease indication and cellular characteristics.<sup>11</sup> Overall, CAR T cell persistence is thus the net outcome of a multifactorial event.<sup>28</sup>

### RESOURCE AVAILABILITY

#### Lead contact

Further information and requests for resources and reagents should be directed to, and will be fulfilled by, the lead contact Sonja Schrepfer ([sonja.schrepfer@sana.com](mailto:sonja.schrepfer@sana.com)).

#### Materials availability

This study did not generate new unique reagents.

#### Data and code availability

This manuscript did not generate any new code. All data reported in this paper will be shared by the [lead contact](#) upon request. Any additional information required to reanalyze the data reported in this paper is available from the [lead contact](#) upon request.

### ACKNOWLEDGMENTS

We thank Tia Arena, Gorman Chen, Amare Lesanework, Steven Long, Dominic Marconi, Lei Wang, and Ryan Zolyomi for Viral Vector Process Develop-

ment and Sylvia Cooley and Henry Vilas for Cell Therapy Process Development. Thanks also to Yunshi Zhou for Cryopreservation Process Development and Lu Dai, Chen Li, Jaclyn Lock, Michelle Polen, and Michael Solomon for supporting as QC Analysts as well as to Diane Wolfe for external manufacturing. Special thanks to Misbah Zafar for T cell culture and support with T cell generation and Carolin Caruso for subpopulation cell cultures.

### AUTHOR CONTRIBUTIONS

X.H. performed all immunobiology and molecular biology experiments and analyzed the data. P.B. and A.W. led the work to generate the cellular intermediates, the final SC291 drug product, and the described subpopulations of SC291. C.W. performed *in vitro* assays. T.D. evaluated the data, developed and produced the figures, and co-wrote the manuscript with S.S. S.S. conceptualized and designed the experiments, supervised the project, and co-wrote the manuscript with T.D. All authors helped edit the manuscript. ARDENT and GLEAM investigators ([Table S2](#)) enrolled the patients and are listed in the supplement together with the ARDENT/GLEAM study organizations ([Table S3](#)).

### DECLARATION OF INTERESTS

All experiments were conducted by or on behalf of Sana Biotechnology, Inc., and no data from UCSF were used. T.D. performed the work in this manuscript as a consultant to Sana Biotechnology, Inc. T.D. owns stock in Sana Biotechnology, Inc. All other authors are employees of and own stock in Sana Biotechnology, Inc. S.S. is an inventor on a patent application covering the study of this publication.

### STAR★METHODS

Detailed methods are provided in the online version of this paper and include the following:

- [KEY RESOURCES TABLE](#)
- [EXPERIMENTAL MODEL AND STUDY PARTICIPANT DETAILS](#)
  - Patients
  - Data analysis
- [METHOD DETAILS](#)
  - SC291 generation
  - Generation of WT CAR T cells, DKO cells, and HIP CAR T cells for *in vitro* assays
  - Cell Sorting of patient's PBMCs
  - Flow Cytometry
  - Elispot
  - Donor specific antibodies (DSA)
  - XCelligence
  - Total IgE Elisa
- [QUANTIFICATION AND STATISTICAL ANALYSIS](#)

### SUPPLEMENTAL INFORMATION

Supplemental information can be found online at <https://doi.org/10.1016/j.stem.2025.07.009>.

(C) IgG DSAs against the three cell fractions of SC291 were quantified by flow cytometry and expressed as mean fluorescence intensity (MFI).

(D) Patient T cell activation by the three cell fractions of SC291 was assessed in ELISpot assays and is expressed as spot frequency.

(E) The cytotoxicity of patient T cells against the three cell fractions of SC291 was assessed in impedance cytotoxicity assays. One sample at 28 days (patient blue) did not contain enough T cells for the assay.

(F) The cytotoxicity of patient NK cells against the three cell fractions of SC291 was assessed in impedance cytotoxicity assays.

(G) For ADCC assays against the three cell fractions of SC291, patient NK cells and serum were combined and killing was assessed in impedance cytotoxicity assays. One sample at 28 days (patient blue) did not contain enough NK cells for the assay.

(H) For CDC assays against the three cell fractions of SC291, patient serum was used in impedance cytotoxicity assays. This group comprised 6 patients. Patients are color coded and all individual patient data are shown.

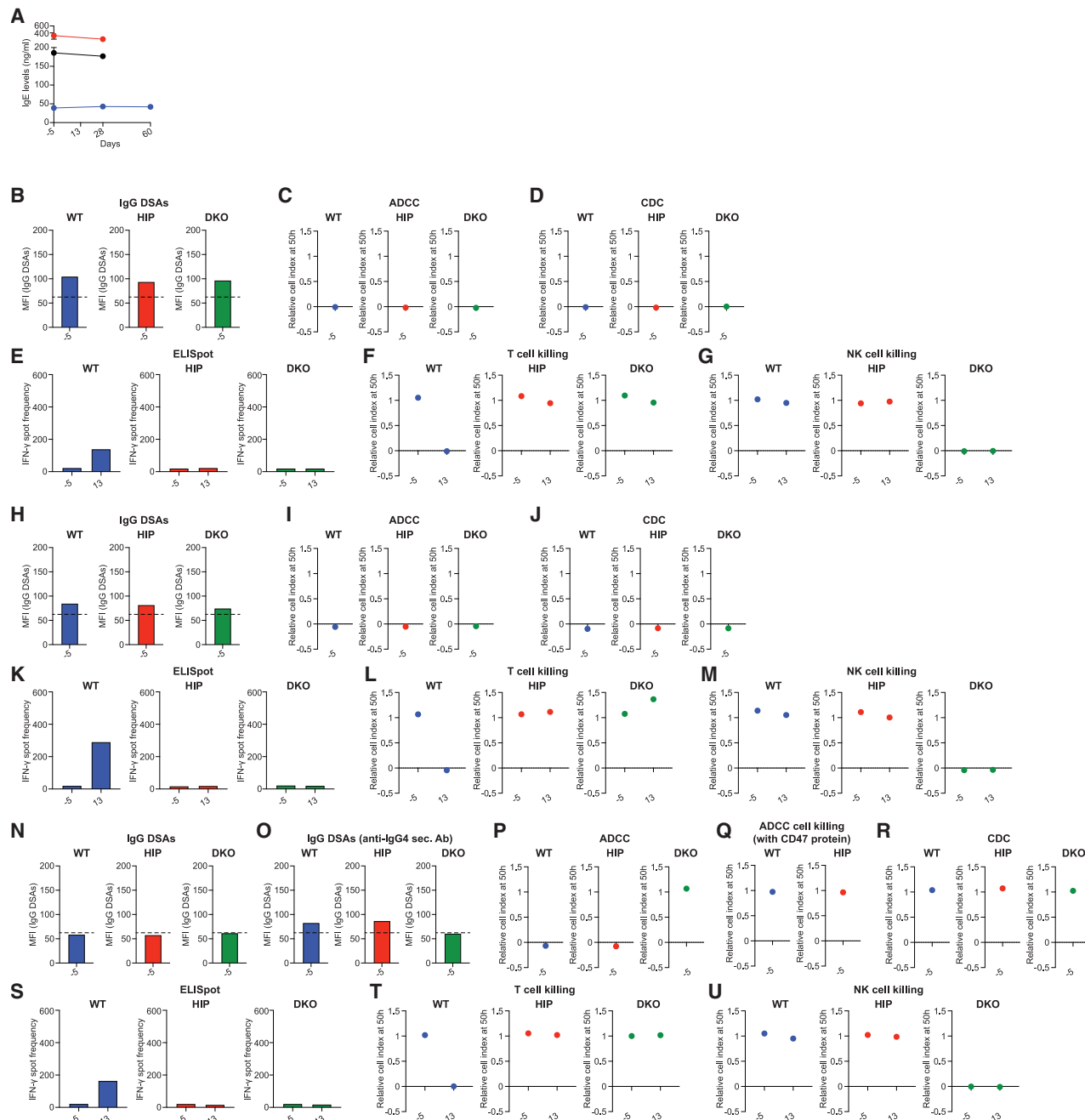


**Figure 6. Patients with baseline killing of HIP CAR T cells**

(A) Circulating IgE levels are shown over time.

(B-G) The first patient. Preformed DSAs against all three cell fractions were observed on day -5 (B). Both ADCC (C) and CDC (D) showed cytotoxicity against all three cell fractions of SC291 even before the treatment was started. But there was no pre-established T cell response against the three cell fractions of SC291 (E) and (F) and NK cells only killed DKO cells (G).

(H-M) The second patient. Preformed DSAs against all three cell fractions were observed on day -5 (H). Both ADCC (I) and CDC (J) showed cytotoxicity against all three cell fractions of SC291 even before the treatment was started. But there was no pre-established T cell response against the three cell fractions of SC291 (K) and (L) and NK cells only killed DKO cells (M).

(N-U) The third patient. Preformed DSAs against WT CAR T cells and HIP CAR T cells were not observed using the regular secondary antibody with preferred affinity for IgG1 (N) but became detectable when a secondary antibody with high affinity for IgG4 was used (O). These IgG4 antibodies mediated ADCC killing of the WT and HIP CAR T cells (P). ADCC killing, however, could be averted when recombinant CD47 was added to the assays (Q). The IgG4 antibodies did not mediate CDC (R). There was no pre-established T cell response against the three cell fractions of SC291 (S) and (T) and NK cells only killed DKO cells (U). See also Figures S2 and S3.

Received: March 11, 2025

Revised: May 30, 2025

Accepted: July 17, 2025

Published: August 13, 2025

## REFERENCES

1. Lipsitz, Y.Y., Timmins, N.E., and Zandstra, P.W. (2016). Quality cell therapy manufacturing by design. *Nat. Biotechnol.* 34, 393–400. <https://doi.org/10.1038/nbt.3525>.
2. Simaria, A.S., Hassan, S., Varadaraju, H., Rowley, J., Warren, K., Vanek, P., and Farid, S.S. (2014). Allogeneic cell therapy bioprocess economics and optimization: single-use cell expansion technologies. *Biotechnol. Bioeng.* 111, 69–83. <https://doi.org/10.1002/bit.25008>.
3. DiNofia, A.M., and Grupp, S.A. (2021). Will allogeneic CAR T cells for CD19 (+) malignancies take autologous CAR T cells 'off the shelf'? *Nat. Rev. Clin. Oncol.* 18, 195–196. <https://doi.org/10.1038/s41571-021-00485-1>.
4. Moradi, V., Omidkhoda, A., and Ahmadbeigi, N. (2023). The paths and challenges of "off-the-shelf" CAR-T cell therapy: An overview of clinical trials. *Biomed. Pharmacother.* 169, 115888. <https://doi.org/10.1016/j.bioph.2023.115888>.
5. Mansoori, S., Noei, A., Maali, A., Seyed-Motahari, S.S., and Sharifzadeh, Z. (2024). Recent updates on allogeneic CAR-T cells in hematological malignancies. *Cancer Cell Int.* 24, 304. <https://doi.org/10.1186/s12935-024-03479-y>.
6. Hering, B.J., Clarke, W.R., Bridges, N.D., Eggerman, T.L., Alejandro, R., Bellin, M.D., Chaloner, K., Czarniecki, C.W., Goldstein, J.S., Hunsicker, L.G., et al. (2016). Phase 3 Trial of Transplantation of Human Islets in Type 1 Diabetes Complicated by Severe Hypoglycemia. *Diabetes Care* 39, 1230–1240. <https://doi.org/10.2337/dc15-1988>.
7. Ramzy, A., Thompson, D.M., Ward-Hartstone, K.A., Ivison, S., Cook, L., Garcia, R.V., Loyal, J., Kim, P.T.W., Warnock, G.L., Levings, M.K., et al. (2021). Implanted pluripotent stem-cell-derived pancreatic endoderm cells secrete glucose-responsive C-peptide in patients with type 1 diabetes. *Cell Stem Cell* 28, 2047–2061.e5. <https://doi.org/10.1016/j.stem.2021.10.003>.
8. Kawamura, T., Ito, Y., Ito, E., Takeda, M., Mikami, T., Taguchi, T., Mochizuki-Oda, N., Sasai, M., Shimamoto, T., Nitta, Y., et al. (2023). Safety confirmation of induced pluripotent stem cell-derived cardiomyocyte patch transplantation for ischemic cardiomyopathy: first three case reports. *Front. Cardiovasc. Med.* 10, 1182209. <https://doi.org/10.3389/fcvm.2023.1182209>.
9. Diorio, C., Teachey, D.T., and Grupp, S.A. (2025). Allogeneic chimeric antigen receptor cell therapies for cancer: progress made and remaining roadblocks. *Nat. Rev. Clin. Oncol.* 22, 10–27. <https://doi.org/10.1038/s41571-024-00959-y>.
10. Martin, K.E., Hammer, Q., Perica, K., Sadelain, M., and Malmberg, K.J. (2024). Engineering immune-evasive allogeneic cellular immunotherapies. *Nat. Rev. Immunol.* 24, 680–693. <https://doi.org/10.1038/s41577-024-01022-8>.
11. Wellhausen, N., Baek, J., Gill, S.I., and June, C.H. (2024). Enhancing cellular immunotherapies in cancer by engineering selective therapeutic resistance. *Nat. Rev. Cancer* 24, 614–628. <https://doi.org/10.1038/s41568-024-00723-5>.
12. Hotta, A., Schrepfer, S., and Nagy, A. (2024). Genetically engineered hypoimmunogenic cell therapy. *Nat. Rev. Bioeng.* 2, 960–979. <https://doi.org/10.1038/s44222-024-00219-9>.
13. Bashor, C.J., Hilton, I.B., Bandukwala, H., Smith, D.M., and Veiseh, O. (2022). Engineering the next generation of cell-based therapeutics. *Nat. Rev. Drug Discov.* 21, 655–675. <https://doi.org/10.1038/s41573-022-00476-6>.
14. Grattoni, A., Korbutt, G., Tomei, A.A., García, A.J., Pepper, A.R., Stabler, C., Brehm, M., Papas, K., Citro, A., Shirwan, H., et al. (2025). Harnessing cellular therapeutics for type 1 diabetes mellitus: progress, challenges, and the road ahead. *Nat. Rev. Endocrinol.* 21, 14–30. <https://doi.org/10.1038/s41574-024-01029-0>.
15. Deuse, T., Hu, X., Gravina, A., Wang, D., Tediashvili, G., De, C., Thayer, W.O., Wahl, A., Garcia, J.V., Reichenspurner, H., et al. (2019). Hypoimmunogenic derivatives of induced pluripotent stem cells evade immune rejection in fully immunocompetent allogeneic recipients. *Nat. Biotechnol.* 37, 252–258. <https://doi.org/10.1038/s41587-019-0016-3>.
16. Deuse, T., Hu, X., Agbor-Enoh, S., Jang, M.K., Alawi, M., Saygi, C., Gravina, A., Tediashvili, G., Nguyen, V.Q., Liu, Y., et al. (2021). The SIRPalpha-CD47 immune checkpoint in NK cells. *J. Exp. Med.* 218, e20200839. <https://doi.org/10.1084/jem.20200839>.
17. Hu, X., Gattis, C., Olroyd, A.G., Friera, A.M., White, K., Young, C., Basco, R., Lamba, M., Wells, F., Ankala, R., et al. (2023). Human hypoimmune primary pancreatic islets avoid rejection and autoimmunity and alleviate diabetes in allogeneic humanized mice. *Sci. Transl. Med.* 15, eadg5794. <https://doi.org/10.1126/scitranslmed.adg5794>.
18. Hu, X., White, K., Olroyd, A.G., DeJesus, R., Dominguez, A.A., Dowdle, W.E., Friera, A.M., Young, C., Wells, F., Chu, E.Y., et al. (2024). Hypoimmune induced pluripotent stem cells survive long term in fully immunocompetent, allogeneic rhesus macaques. *Nat. Biotechnol.* 42, 413–423. <https://doi.org/10.1038/s41587-023-01784-x>.
19. Hu, X., Manner, K., DeJesus, R., White, K., Gattis, C., Ngo, P., Bandoro, C., Tham, E., Chu, E.Y., Young, C., et al. (2023). Hypoimmune anti-CD19 chimeric antigen receptor T cells provide lasting tumor control in fully immunocompetent allogeneic humanized mice. *Nat. Commun.* 14, 2020. <https://doi.org/10.1038/s41467-023-37785-2>.
20. Hu, X., White, K., Young, C., Olroyd, A.G., Kievit, P., Connolly, A.J., Deuse, T., and Schrepfer, S. (2024). Hypoimmune islets achieve insulin independence after allogeneic transplantation in a fully immunocompetent non-human primate. *Cell Stem Cell* 31, 334–340.e5. <https://doi.org/10.1016/j.stem.2024.02.001>.
21. Bai, Z., Feng, B., McClory, S.E., de Oliveira, B.C., Diorio, C., Gregoire, C., Tao, B., Yang, L., Zhao, Z., Peng, L., et al. (2024). Single-cell CAR T atlas reveals type 2 function in 8-year leukaemia remission. *Nature* 634, 702–711. <https://doi.org/10.1038/s41586-024-07762-w>.
22. Horowitz, A., Strauss-Albee, D.M., Leipold, M., Kubo, J., Nemat-Gorgani, N., Dogan, O.C., Dekker, C.L., Mackey, S., Maecker, H., Swan, G.E., et al. (2013). Genetic and environmental determinants of human NK cell diversity revealed by mass cytometry. *Sci. Transl. Med.* 5, 208ra145. <https://doi.org/10.1126/scitranslmed.3006702>.
23. LeBien, T.W., and Tedder, T.F. (2008). B lymphocytes: how they develop and function. *Blood* 112, 1570–1580. <https://doi.org/10.1182/blood-2008-02-078071>.
24. Bruhns, P., Iannascoli, B., England, P., Mancardi, D.A., Fernandez, N., Jorieux, S., and Daëron, M. (2009). Specificity and affinity of human Fc $\gamma$  receptors and their polymorphic variants for human IgG subclasses. *Blood* 113, 3716–3725. <https://doi.org/10.1182/blood-2008-09-179754>.
25. Freitas Monteiro, M., Papaserafeim, M., Réal, A., Puga Yung, G.L., and Seebach, J.D. (2020). Anti-CD20 rituximab IgG1, IgG3, and IgG4 but not IgG2 subclass trigger Ca(2+) mobilization and cytotoxicity in human NK cells. *J. Leukoc. Biol.* 108, 1409–1423. <https://doi.org/10.1002/JLB.5MA0620-039R>.
26. Damelang, T., de Taeye, S.W., Rentenaar, R., Roya-Kouchaki, K., de Boer, E., Derkzen, N.I.L., van Kessel, K., Lissenberg-Thunnissen, S., Rooijakkers, S.H.M., Jongerius, I., et al. (2023). The Influence of Human IgG Subclass and Allotype on Complement Activation. *J. Immunol.* 211, 1725–1735. <https://doi.org/10.4049/jimmunol.2300307>.
27. Tao, M.H., Smith, R.I., and Morrison, S.L. (1993). Structural features of human immunoglobulin G that determine isotype-specific differences in complement activation. *J. Exp. Med.* 178, 661–667. <https://doi.org/10.1084/jem.178.2.661>.
28. Deuse, T., and Schrepfer, S. (2025). Progress and challenges in developing allogeneic cell therapies. *Cell Stem Cell* 32, 513–528. <https://doi.org/10.1016/j.stem.2025.03.004>.

29. Labanieh, L., and Mackall, C.L. (2023). CAR immune cells: design principles, resistance and the next generation. *Nature* 614, 635–648. <https://doi.org/10.1038/s41586-023-05707-3>.
30. Biasco, L., Izotova, N., Rivat, C., Ghorashian, S., Richardson, R., Guvenel, A., Hough, R., Wynn, R., Popova, B., Lopes, A., et al. (2021). Clonal expansion of T memory stem cells determines early anti-leukemic responses and long-term CAR T cell persistence in patients. *Nat. Cancer* 2, 629–642. <https://doi.org/10.1038/s43018-021-00207-7>.
31. Bai, Z., Woodhouse, S., Zhao, Z., Arya, R., Govek, K., Kim, D., Lundh, S., Baysoy, A., Sun, H., Deng, Y., et al. (2022). Single-cell antigen-specific landscape of CAR T infusion product identifies determinants of CD19-positive relapse in patients with ALL. *Sci. Adv.* 8, eabj2820. <https://doi.org/10.1126/sciadv.abj2820>.
32. Stadtmauer, E.A., Fraietta, J.A., Davis, M.M., Cohen, A.D., Weber, K.L., Lancaster, E., Mangan, P.A., Kulikovskaya, I., Gupta, M., Chen, F., et al. (2020). CRISPR-engineered T cells in patients with refractory cancer. *Science* 367, eaba7365. <https://doi.org/10.1126/science.aba7365>.
33. Tang, N., Cheng, C., Zhang, X., Qiao, M., Li, N., Mu, W., Wei, X.F., Han, W., and Wang, H. (2020). TGF-beta inhibition via CRISPR promotes the long-term efficacy of CAR T cells against solid tumors. *JCI Insight* 5, e133977. <https://doi.org/10.1172/jci.insight.133977>.
34. Wei, J., Long, L., Zheng, W., Dhungana, Y., Lim, S.A., Guy, C., Wang, Y., Wang, Y.D., Qian, C., Xu, B., et al. (2019). Targeting REGNASE-1 programs long-lived effector T cells for cancer therapy. *Nature* 576, 471–476. <https://doi.org/10.1038/s41586-019-1821-z>.

**STAR★METHODS**

**KEY RESOURCES TABLE**

REAGENT or RESOURCE	SOURCE	IDENTIFIER
<b>Antibodies</b>		
FITC-labeled CD47 antibody	Biolegend	Cat#323106, clone CC2C6; RRID:AB_756136
APC-labeled HLA-A,B,C antibody	BD Biosciences	Cat#555555, clone G46_2.6; RRID:AB_398603
AF647-labeled anti-HLA-DR,DP,DQ antibody	BD Biosciences	Cat#563591, clone Tu39; RRID:AB_2738298
AF488-labeled CD3 antibody	Biolegend	Cat#300415, clone UCHT1; RRID:AB_389310
PerCP-Cy5.5-labeled CD56 antibody	Biolegend	Cat#304626, clone MEM-188; RRID:AB_10641700
APC-labeled CD19 antibody	Biolegend	Cat#302212, clone HIB19; RRID:AB_314242
FITC-conjugated rabbit anti-human IgG antibody	Sigma Aldrich	Cat#F4512; RRID:AB_259601
FITC-conjugated rabbit anti-human IgG4 antibody	AssayPro	Cat#34108-0514
<b>Chemicals, peptides, and recombinant proteins</b>		
Human recombinant IL-2	Akron Bio	PN AK8223-0100
Collagen	Sigma-Aldrich	Cat#C3867
Fibronectin	Sigma Aldrich	Cat#S517
Laminin	Gibco	Cat#A29249
Human recombinant IL-2	Peprotech	Cat# 200-02
Human recombinant CD47	BPS BioScience	Cat#71177
<b>Critical commercial assays</b>		
Human IFN- $\gamma$ ELISpot assays	BD Bioscience	Cat#551849,
Total IgE ELISA kit	Abcam	Cat#ab195216
<b>Software and algorithms</b>		
Prism 10	GraphPad	N/A
<b>Other</b>		
Selection Buffer (CliniMACS® PBS/EDTA Buffer)	Miltenyi Biotec	PN 200-070-022
HSA	Octapharma	PN 68982-0643-01
CliniMACS® CD8 Reagent	Miltenyi Biotec	PN 200-070-215
CliniMACS® CD4 Reagent	Miltenyi Biotec	PN 200-070-213
Washing Buffer (PlasmaLyte A)	Baxter	PN 0338-0221-04
CS10	BioLife Solutions	PN 210202
CTS™ Dynabeads™	Thermo Fisher Scientific	PN 40203D
CliniMACS® CD3 Reagent	Miltenyi Biotec	PN 200-070-202
HRP Streptavidin	BD Bioscience	Cat#557630
AEC Substrate Solution	BD Bioscience	Cat#551951

**EXPERIMENTAL MODEL AND STUDY PARTICIPANT DETAILS**

**Patients**

All patients from the ARDENT trial (NCT05878184) and GLEAM trial (NCT06294236) who had immune response data available on the cut-off date of September 19, 2024 were included. Inclusion and exclusion criteria were as follows:

**ARDENT**

Inclusion Criteria:

- Male or female subjects aged 18-80 years at the time of signing informed consent.
- Diagnosis of NHL (WHO 2016 criteria) or CLL (iwCLL criteria), including:
- Large B-cell lymphoma, including diffuse large B-cell lymphoma (DLBCL) not otherwise -- specified (including DLBCL arising from indolent lymphoma), primary mediastinal large -- B-cell lymphoma, high grade B-cell lymphoma, follicular lymphoma grade 3B
- Follicular lymphoma (dose escalation only except for follicular lymphoma grade 3B)

- Marginal zone lymphoma (dose escalation only)
- Mantle cell lymphoma (dose escalation only)
- CLL or SLL
- Relapsed/refractory disease after at least 2 prior systemic regimens per standard of care or after autologous stem cell transplant
- ECOG performance status of 0 or 1.
- At least one measurable lesion per Lugano Classification (NHL); CLL subjects must meet iwCLL treatment criteria
- Life expectancy  $\geq 12$  weeks

**Exclusion Criteria:**

- Prior anti-CD19 therapy including CD19-directed CAR T treatment or other CD19-directed antibody or cell therapy (e.g., NK cell). (Part 2 dose expansion only - prior approved CD19-directed CAR T therapy required)
- History of primary central nervous system (CNS) lymphoma or presence of CNS metastases
- Systemic anticancer therapy (including platinum-based chemotherapies and I/O therapies) or radiotherapy within 14 days of SC291 (28 days for biologics)
- Autologous HSCT within 6 weeks of treatment with SC291 (or allogeneic HSCT at any time).
- Active autoimmune disease or any other diseases requiring immunosuppressive therapy or corticosteroid therapy (defined as  $>20$  mg/day prednisone or equivalent).
- History or presence of cardiac or CNS disorders as defined in the protocol

**GLEAM**

**Inclusion Criteria:**

1. Age  $\geq 18$  and  $\leq 75$
2. For LN cohort:
  - o Diagnosis of SLE based on the 2019 European League Against Rheumatism (EULAR)/American College of Rheumatology (ACR)
  - o Biopsy-proven LN class III or IV, according to 2018 Revised International Society of Nephrology/Renal Pathology Society (ISN/RPS) criteria
  - o Refractory disease to  $\geq 2$  prior treatment regimens
3. For ERL cohort:
  - o Diagnosis of SLE based on the 2019 European League Against Rheumatism (EULAR)/American College of Rheumatology (ACR) classification criteria for adult SLE
  - o Severe or relapsing disease not responding to at least 2 prior recent disease-modifying therapies
4. For AAV Cohort, diagnosed with Granulomatous Polyangiitis (GPA) or Microscopic Polyangiitis (MPA) based on the 2022 ACR/EULAR classification criteria

**Exclusion Criteria:**

1. Prior CD19-directed cell therapy including CAR T treatment or other genetically modified cell therapy (e.g., Natural Killer (NK) cell)
2. For LN and ERL Cohorts, central nervous system (CNS) lupus manifestations or history or presence of CNS disorder
3. For LN and ERL Cohorts, diagnosis of anti-phospholipid antibody syndrome
4. For AAV Cohort only, Diagnosis of Eosinophilic Granulomatosis with Polyangiitis (EGPA) as defined by the 2022 ACR/EULAR classification criteria for EGPA

**Data analysis**

These data were presented at the 5<sup>th</sup> IPITA / HSCI / JDRF Summit October 28–29, 2024 in Boston. The data analysis was in accordance with both the ARDENT and GLEAM Clinical Study Protocols.

**METHOD DETAILS**

**SC291 generation**

Peripheral mononuclear cells with 150 mL of autologous plasma were collected from a 20-year-old female donor of blood type O by apheresis using the Spectra Optia® Apheresis System (leukopak from HemaCare, PN PB001F-1). The leukopak was shipped to the manufacturing site in a temperature-controlled shipper (2–8°C). The leukopak was washed with Selection Buffer (CliniMACS® PBS/EDTA Buffer, Miltenyi Biotec, PN 200-070-022), supplemented with 0.5% HSA (Octapharma, PN 68982-0643-01). CD8<sup>+</sup> and CD4<sup>+</sup> cells were serially isolated within 36 hours of the collection, first by purifying CD8<sup>+</sup> cells directly from the apheresis product using the Clinimacs® CD8 Reagent (Miltenyi Biotec, PN 200-070-215) and Clinimacs® Plus instrument, and then by purifying CD4<sup>+</sup> cells

from the negative CD8<sup>+</sup> selection fraction, using the CliniMACS® CD4 Reagent (Miltenyi Biotec, PN 200-070-213) and CliniMACS® Plus instrument. Following purification, the CD4<sup>+</sup> and CD8<sup>+</sup> cellular intermediates were washed with Washing Buffer (PlasmaLyte A, Baxter, PN 0338-0221-04) supplemented with 1.2% HSA (Octapharma, PN 68982-0643-01), and then diluted with CS10 (BioLife Solutions, PN 210202) to achieve a 3:1 CryoStor® CS10 (Biolife Solutions)-to-Washing Buffer (Plasmalyte A + 1.2% HSA) composition. The formulated cellular intermediates were filled into cryobags (Charter Medical, PN FP-FLEX500B), individually cryopreserved, and stored at <-150°C until further processing.

The CD4 and CD8 cellular intermediates were thawed (Biolife Solutions, ThawSTAR CB) and washed with culture media supplemented with 100 IU/ml recombinant human IL-2 (Akron Bio, PN AK8223-0100). The cells were then combined at a 1:1 CD4:CD8 ratio, activated using CTS™ Dynabeads™ (Thermo Fisher Scientific, PN 40203D), and cultured in a rocking motion bioreactor (Cytiva, Xuri W25) at 37.0°C, 5.0% CO<sub>2</sub> balance air overlay. On day 1, the cells were transduced by spinoculation at 1,000 g for 90 minutes (Cytiva, Sepax C-Pro) with bicistronic lentiviral vectors (LVV) delivering the EF1 $\alpha$ -driven CD47-2A-CD19CAR transgenes. The volume of LVV used was determined via functional titration. Cells were cultured until day 3 when the activation beads were removed (CTS™ DynaMag™ Magnet, Life Technologies). The cells were concentrated by counterflow centrifugation (CTS™ Rotea™, Life Technologies), and gene edited by electroporation using the MaxCyte ExPERT GTx™ (Expanded T Cell 1 Program, CL-2™ GMP flow-through electroporation cassette) with Cas12b mRNA and guide RNAs targeting the T cell receptor alpha constant (*TRAC*), beta-2-microglobulin (*B2M*), and the class II major histocompatibility complex transactivator (*CIITA*). Cells were cultured until day 7, when the cells were removed from the bioreactor, washed, and concentrated (Fresenius Kabi, Lovo® Automated Cell Processing System), incubated with the CliniMACS® CD3 Reagent (Miltenyi Biotec, PN 200-070-202) per the manufacturer's recommendation followed by depleting the CD3 cells using the CliniMACS® Plus. The purified cells were cultured for an additional 2 days. On day 9, cells were harvested and washed using Washing Buffer (PlasmaLyte A + 1.2% HSA) using the Lovo®, formulated in cryoformulation media by adding CryoStor® CS10 to achieve a 3:1 CS10:Washing Buffer composition, filled in AT-Closed Vials® (Aseptic Technologies), and cryopreserved in a controlled rate freezer. The viral copy number (VCN) of the SC291 drug product was 2.7. Drug product characteristics are shown in Table 1. The frequency of HIP CAR T cells was measured by direct flow co-gating for live TCR-negative, HLA-ABC-negative, HLA-DR,DP,DQ-negative, CD47 high, and CD19CAR-positive cells and thus slightly differs from a calculated value based on the product of the frequencies of each individual population. The cryopreserved cells were stored at <-150°C. All patients in this study received the same SC291 drug product.

### Generation of WT CAR T cells, DKO cells, and HIP CAR T cells for in vitro assays

CD4 and CD8 cellular intermediates were thawed, washed, and activated using CTS™ Dynabeads™ (Thermo Fisher Scientific, PN 40203D). WT CAR T cells were produced by transducing activated T cells with the CD47-2A-CD19CAR LVV one day post-activation as described above, followed by culture until 9 days post-activation. Cells were incubated with FITC-labeled CD47 antibody (cat. 323106, clone CC2C6, Biolegend) and sorted for CD47 positive cells.

DKO cells were produced by introducing Cas12b mRNA and guide RNAs via electroporation into T cells 3 days post-activation as described above, followed by culture until 9 days post-activation. DKO cells were incubated with APC-labeled HLA-A,B,C (cat. 555555, clone G46\_2.6, BD Biosciences) and AF647-labeled anti-HLA-DR,DP,DQ antibody (cat. 563591, clone Tu39, BD Biosciences) and flow sorted for double negative cells (BD Aria Fusion, Franklin Lakes, NJ). HIP CAR T cells were isolated from the SC291 drug product via sorting using APC-labeled HLA-A,B,C (cat. 555555, clone G46\_2.6, BD Biosciences), AF647-labeled anti-HLA-DR,DP,DQ antibody (cat. 563591, clone Tu39, BD Biosciences) and FITC-labeled CD47 antibody (cat. 323106, clone CC2C6, Biolegend) and sorted for HLA-A,B,C and HLA-DR,DP,DQ double negative cells and CD47 positive cells (BD Aria Fusion). Cells were formulated in cryoformulation media by adding CryoStor® CS10 to achieve a 3:1 CS10:Washing Buffer (PlasmaLyte A + 1.2% HSA) composition and cryopreserved in a controlled rate freezer. The cryopreserved cells were stored at <-150°C.

### Cell Sorting of patient's PBMCs

Patient's PBMC samples were thawed, pooled and counted with an automated thawing system (Thaw star, Stemcell Technologies, Vancouver, Canada) and stained with AF488-labeled CD3 (cat. 300415, clone UCHT1, Biolegend), and PerCP-Cy5.5-labeled CD56 (cat. 304626, clone MEM-188, Biolegend) antibodies. Cell sorting was performed for CD3 positive cells T cells and CD3 negative and CD56 positive natural killer (NK) cells using BD FACS Aria Fusion.

### Flow Cytometry

For the detection of CD19 positive cells, 1 million of patient's PBMCs were stained with APC-labeled CD19 antibody (cat. 302212, clone HIB19, Biolegend) for 45 min at 4°C and analyzed using BD FACS Aria Fusion. Data were analyzed in FlowJo 10.8.2. The CD19 cell fraction was expressed as percentage of PBMCs.

### Elispot

Human IFN- $\gamma$  ELISpot assays (cat. 551849, BD Bioscience) were performed with WT CAR-T, DKO cells, or HIP CAR-T cells as stimulator cells after mitomycin-treatment with 50  $\mu$ g/ml for 30 min and patient's T-cells as responder cells. One hundred thousand stimulator cells were incubated with one hundred thousand recipient responder for 48 hours and incubated with HRP Streptavidin (cat. 557630, BD Bioscience). Spots were developed using AEC Substrate Solution (cat. 551951, BD Bioscience) and IFN- $\gamma$  spot frequencies were enumerated using an Elispot plate reader (AID Diagnostika GmbH, Strassberg, Germany).

### Donor specific antibodies (DSA)

Patient serum samples were decomplemented at 56 °C for 30 minutes. Equal amounts of sera and cell suspensions at  $5 \times 10^6$  per ml were incubated for 45 min at 4 °C. Afterwards, cells were labeled with FITC-conjugated rabbit anti-human IgG (cat. F4512, polyclonal, Sigma Aldrich) or FITC-conjugated rabbit anti-human IgG4 (cat. 34108-0514, polyclonal, AssayPro) for another 45 min at 4 °C. Mean fluorescence intensity was analyzed by flow cytometry (Attune, Thermo Fisher).

### XCelligence

Human T cell and NK cell killing assays were performed on the XCelligence MP platform (Agilent, Santa Clara, CA). Specialized 96-well E-plates (ACEA BioSciences) were coated with a mixture of collagen (cat. C3867, Sigma-Aldrich), fibronectin (cat. S517, Sigma Aldrich) and laminin (cat. A29249, Gibco). Forty thousand target cells were plated in 100 µl media. After the cell Index reached 0.7, the effector cells were added at an effector cell to target cell (E:T) ratio of 1:1. NK cells were stimulated with 1 µg/ml human IL-2 and T cells with 100 ng/ml human IL-2 (Peprotech).

CDC and ADCC killing assays were also performed on the XCelligence MP platform. For CDC assays, 100 µl of untreated, complement-containing serum (1:1 mixed with media) was added. For ADCC assays, 50 µl heat-inactivated serum with  $4 \times 10^4$  human NK cells were added. In some conditions, recombinant CD47 was added at a concentration of 1 µl/ml (cat. 71177, BPS BioScience). As killing control, target cells were treated with 2% TritonX100. As survival control, cells were only incubated with media. All cell index data were normalized to those of control wells containing only the target cells. A relative cell index of 1 at 50 h thus corresponds with optimal survival and a relative cell index at 50 h of 0 means target cell death. Data were analyzed with the RTCA software (Agilent). The blue patient in Figure 5 is missing 28-day data for T cell killing and ADCC because not enough sample was received.

### Total IgE Elisa

The Total IgE ELISA kit (cat. ab195216, Abcam, Cambridge, UK) was used to measure total IgE in patient's serum. Samples were diluted 1:800 and pipetted according to manufacturer's instructions. Briefly, standards or samples were added to the 96-well ELISA plate along with the provided antibody cocktail and incubated for 1 hour. After washing, TMB Substrate was added to each well and incubate for 10 minutes in the dark on a plate shaker set to 400 rpm. Then, 100 µl of Stop Solution was added to each well. Samples were analyzed in a microplate reader at 450 nm (Perkin – Elmer).

### QUANTIFICATION AND STATISTICAL ANALYSIS

GraphPad Prism 10 was used for graphs. Fisher's exact test was used to compare categorical variables across two or three groups. The Mann Whitney test with exact *P* values was used to compare continuous variables between two groups. All *P* values are presented in the figures.